Climate Dynamics (2004) 22: 795–814
DOI 10.1007/s00382-004-0418-9

E. Aldrian · L. Dümenil-Gates · D. Jacob · R. Podzun
D. Gunawan

Long-term simulation of Indonesian rainfall with the MPI regional model

Received: 17 June 2003 / Accepted: 16 February 2004 / Published online: 13 May 2004

Abstract Simulations of the Indonesian rainfall variability using the Max Planck Institute regional climate model REMO have been performed using three different lateral boundary forcings: Reanalyses from the European Centre for Medium-Range Weather Forecasts (ERA15), the National Centers for Environmental Prediction and National Center for Atmospheric Research (NRA) as well as from ECHAM4 climate model simulation. The result of those simulations are compared to station data. REMO simulations were performed at 0.5° horizontal resolution for the whole archipelago and at 1/6° for Sulawesi Island. In general the REMO model, reproduces the spatial pattern of monthly and seasonal rainfall well over land, but overestimates the rainfall over sea. Superiority of REMO performance over land is due to a high-resolution orography, while over sea, REMO suffers from erroneously low surface fluxes. REMO reproduces variability during El Niño-Southern Oscillations years well but fails to show a good (wet and dry) monsoon contrast. Despite strong influences of the lateral boundary fields, REMO shows a realistic improvement of a local phenomenon over Molucca. Significant improvement for the step from the relatively high global 1.125° to 0.5° resolution is noticeable, but not from 0.5° into 1/6°. The REMO simulation driven by ERA15 has the best quality, followed by NRA and ECHAM4 driven simulations. The quality of ERA15 is the main factor determining the quality of REMO simulations. A predictability study shows small internal variability among ensemble members. However, there are systematic intrinsic climatological errors as shown in the predictability analysis. These intrinsic errors have monthly, seasonal and regional dependencies and the one over Java is significantly large. The intrinsic error study suggests the presence of the spring predictability barrier and a high level of predictability in summer.

E. Aldrian (✉) · L. Dümenil-Gates · D. Jacob · R. Podzun
Max Planck Institut für Meteorologie,
Bundesstraße 55, 20146 Hamburg, Germany
E-mail: aldrian@eudoramail.com

Present address: E. Aldrian
The Agency for the Assessment and Application of Technology,
BPPT, Jakarta, Indonesia

Present address: L. Dümenil-Gates
National Science Foundation,
4201 Wilson Blvd, Arlington, VA 22230, USA

D. Gunawan
Institute of Bioclimatology,
Georg–August–Universität, Göttingen, Germany

1 Introduction

The Indonesian part of the Asian monsoon has received less attention in comparison to other Asian monsoon areas like India and China. Studies of the monsoon over the region using global and regional climate models are rare. This study is motivated by the inadequate results of the Max Planck Institute's high-resolution ECHAM4 global circulation model (GCM) over Indonesia at T106 (1.125°) resolution (Aldrian et al. 2003). Due to the presence of complex topography and insufficient model resolution in the region, current GCM shows a mediocre performance in simulating the precipitation and its variability in the region. The complexity of the region, especially the land sea representation, requires a high-resolution model. Furthermore, previous studies showed significant improvements of rainfall representation when a moderate resolution was replaced by a higher resolution GCM (Stendel and Roeckner 1998; Jha et al. 2000). Regional modeling (RCM) may allow the high resolution required, but there is no study yet using a regional climate model in the region.

The meteorology of Indonesian rainfall has been described recently by Haylock and McBride (2001); Hamada et al. (2002); Hendon (2003) and Aldrian and

Susanto (2003). Haylock and McBride (2001), using an all-Indonesian rainfall index, found that the wet season of Indonesia is inherently unpredictable. Hamada et al. (2002) and Aldrian and Susanto (2003) indicated three dominant rainfall climatic regions with intermediate regions in between. Both agree on the type of monsoonal climate with the maximum of the annual cycle occurring during December/January/February, whereas in the eastern islands of Molucca the maximum of the annual cycle occurs during May/June/July. All four studies agree on the negative El Niño-Southern Oscillations (ENSO) impact to the Indonesian rainfall (in terms of the correlation between the sea surface temperature, SST, in the Pacific to Indonesian rainfall) especially during the dry period from April to October Hendon 2003; Aldrian and Susanto (2003). El Niño (La Niña) results in a lower (higher) rainfall amount in the dry period.

One possibility for downscaling GCM results to the regional scale is to apply a nested RCM. For reviews of RCM, the readers are referred to Mesinger (1997) and Staniforth (1997). The Max Planck Institute (MPI) regional model REMO (Jacob 2001; Jacob et al. 2001) is suitable for this purpose because REMO provides detailed forecasts of weather parameters close to the ground and an improved simulation of clouds and rainfall compared to a GCM. Regional models are, however, dependent upon the lateral boundary prescription (Warner et al. 1997), which limits their capability in studying long-term climate behavior. The purposes of the study are to show REMO capabilities in simulating the monthly to interannual rainfall variability, to see the downscaling effect at two different resolutions (0.5° and 1/6°), to compare the variability with three different lateral boundaries from the European Centre for Medium-range Weather Forecast (ECMWF) reanalyses (ERA15; Gibson et al. 1997), the National Centers for Environmental Prediction and National Center for Atmospheric Research (NCEP-NCAR) reanalyses (NRA; Kalnay et al. 1996) and the MPI ECHAM4 (Roeckner et al. 1996) simulation and to explore the rainfall predictability with different initial conditions.

This study focuses on the rainfall simulated by REMO. The regional model produces large-scale and convective type precipitation, however due to limited observations, the study focuses mainly on the total rainfall. The time scale is limited to monthly, seasonal and interannual periods from 1979–1993 (except for comparisons with the ECHAM4 GCM, for which simulations are available only from 1979–1988). The outline of this study is as follows. Sect. 2 discusses the data and model setup, Sect. 3 the results of REMO simulations over five major islands and three sea regions with three different boundary forcings, the results of some sensitivity studies to improve the rainfall simulation over the sea, and the results of the down-scaling. Sect. 4 discusses the REMO predictability. Finally, Sect. 5 there is a summary of the main findings.

2 Data and model setup

2.1 Data

The observational data used in this study are monthly rainfall data collected by the Indonesian Meteorological and Geophysical Agency (BMG) at 167 stations all over Indonesia and monthly mean rainfall data from the WMO-NOAA project on the Global Historical Climatology Network (GHCN; Vose et al. 1992) from 1979 to 1993. The data have undergone some quality control tests including the homogeneity test before they are incorporated into GHCN (Vose et al. 1992). In our area of interest (19°S–8°N and 95°E–145°E) there are 545 rain gauges. Their data are gridded onto the REMO grid at 0.5° resolution using the Cressman (1959) method. As the second observational data set, a combination of gauge observations with satellite estimates from the Global Precipitation Climatology Project (GPCP; Huffman et al. 1997) at 1° spatial resolution is used. The data were interpolated onto the REMO grid.

The regional model simulations were driven by lateral boundary conditions interpolated from either of two reanalyses. The first is ERA15 at the horizontal resolutions T106 or equivalent to 1.125° in the tropics, and the second one is the 40-year NCEP reanalysis (NRA) with a fixed spatial resolution of T62 (equivalent to 2.5° in the tropics). The reanalyses data are available at 6 h intervals from 1979 until 1993.

The third lateral boundary condition is taken from the ECHAM4 climate simulation, which was used for a resolution sensitivity study by Stendel and Roeckner (1998). This particular version of the ECHAM4 model is a spectral model with a triangular truncation at the wave number 106 (T106). For the vertical representation a 19 level hybrid sigma-pressure coordinate system is used. The time integration is carried out using a semi-implicit "leapfrog" method. The orography and the land-sea mask are calculated from a high resolution (1 km) US Navy data set. This simulation is part of the Atmospheric Model Intercomparison Project (AMIP; Gates 1992), in which several global atmospheric models participated in simulating climate over 1979–1988. The ECHAM4 model was driven by interannually varying SSTs from the AMIP 2 (Gates et al. 1999) at T106 resolution.

An independent gridded SST data from the Global Ice and Sea Surface Temperature dataset (GISST2; Rayner et al. 1996) version 2.3b are used in this study to validate other SST data. This dataset is compiled from SST observations from 1903 - present, with a spatial resolution of 1°. To confirm with the rainfall data, we use data from 1979 to 1993 only.

2.2 REMO model descriptions

REMO is a hydrostatic model that is either combined with the European Model/Deutschland Model (EM/

DM; Jacob and Podzun 1997) or the ECHAM4 physics parametrization packages (e.g. Jacob 2001). In this study, the physical parametrizations of ECHAM4 were used. The dynamical core of the model as well as the discretization in space and time are based on the European-Model. However, in REMO with ECHAM-4 physics temperature, water vapor and liquid water are prognostic variables instead of enthalpy and total water content. In addition, horizontal wind components and surface pressure are also prognostic variables. The model uses the Arakawa-C grid for the horizontal representation and a hybrid system of p and η using 20 levels in the vertical. Vertical discretization follows Simmons and Burridge (1981). The time discretization uses a semi-implicit leapfrog scheme and an explicit advection scheme. The lateral boundary interpolation uses the method of Davies (1976), where the lateral boundary relaxation zones extend to eight grid rows. The lateral boundary consists of all prognostic variables except the parameters described in Table 1. At the upper boundary a radiative upper boundary condition according to Klemp and Durran (1983) and Bougeault (1983) is applied.

The radiation parametrization is adopted from the ECMWF model (Fouquart and Bonnel 1980; Morcrette and Fouquart 1986) with only a few changes described in Roeckner et al. (1996). The grid-scale parametrization of cloud microphysics is based on the solution of the budget equations with the bulk schemes from Kesler (1969) and the sub grid-scale precipitation processes follow Tiedtke (1989), with deep convection adjustments due to Nordeng (1994). Condensation values are based on Sundqvist (1978).

Clouds are divided into stratiform and convective clouds. The liquid water content of stratiform clouds is determined by the corresponding budget equation including sources and sinks due to phase changes and precipitation. An empirical and temperature dependent function is used to determine the cloud ice content, through which influences on the radiation are included. The parametrisation of the convective clouds is based on the mass flux concept from Tiedtke (1989) with changes in the deep convection.

REMO has three types of convection: penetrative, shallow and mid-level convection. Only one scheme is allowed in a grid cell. Penetrative convection is considered when the cloud base is in the planetary boundary layer and large-scale convergence prevails in the lower troposphere. In shallow convection, the cloud is formed in conditions of a slightly divergent flow and is often driven by evaporation at the surface or over water. In mid-level convection, the cloud has its cloud base in the free atmosphere and occurs together with large-scale lifting in the vicinity of fronts with regions of thermal instability. Penetrative convection is assumed if the dynamic fraction due to advective humidity transport predominates, while shallow convection is assumed if evaporation from the surface (land or ocean) is of larger importance.

In REMO, soil temperatures on land are calculated from diffusion equations solved in five different layers covering the uppermost 10 m of the soil. The global data set of fields of land surfaces is constructed from the major ecosystem complexes of Hagemann et al. (1999). Surface mean orography and variances are calculated from the USGS GTOPO30 topography data with a spatial resolution of 1 km. All surface parameters are constant in time, i.e., do not vary monthly or seasonally. The land surface scheme follows Dümenil and Todini (1992). In this study, only one type of surface cover is present on each grid cell (land, water or ice).

2.3 Model setups

The model was run in the climate mode with lateral boundary conditions from ERA15 (REMO-ERA), NRA (REMO-NRA) and an ECHAM4 simulation (REMO-ECHAM). With the climate mode, a regional model has to be initialized once and uses surface parameters over land, SST over oceans and boundary and using surface lateral boundary values during the whole simulation. The lateral boundaries have a temporal resolution of 6 h and are interpolated into a 5 min time step. A simulation of 15 years (1979–1993) was performed for each reanalysis and a simulation of 10 years (1979–1988) for the ECHAM4 model. Table 1 shows major differences among the three lateral boundary fields. The study was conducted at two horizontal resolutions with 20 hybrid vertical layers each. At the resolution 0.5° (55 km), the model is formulated in a finite difference grid with 101 points in longitude, 55 points in latitude with a bottom left corner at 91°E/19°S. This grid system covers the whole Indonesian archipelago. At the resolution 1/6° (18 km) the model has 63 grid points in longitude and 71 points in latitude with a bottom left corner at 117°E/7°S. The latter grid system covers Sulawesi Island (REMO-1/6) and was driven at the lateral boundary from the output of the REMO-ERA simulation. Figure 1 illustrates the structure of the REMO simulations at the two resolutions.

Table 1 The quality of the three different lateral boundaries

Forcings	Days	Time span	Liquid water content	Specific humidity	Original resolution
ERA15	365	1979–1993	Yes	All layers	1.125
NRA	365	1979–1993	No	Not upper 9 layers	1.875
ECHAM4	360 (Julian)	1979–1988	Yes	All layers	1.125

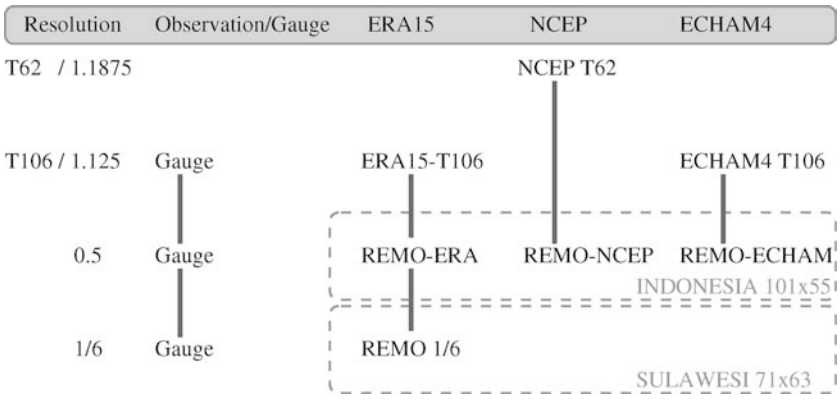

Fig. 1 The experiment setups with three lateral boundaries and two different resolutions

In the predictability analysis, those simulations become the control runs, and six other simulations were performed for REMO-ERA and REMO-ECHAM, which make up two ensembles. Thus each ensemble consists of a control run and six ensemble members, whose initial condition differs from the control run by 12 to 72 h, and each is integrated for 15 years.

3 Results of REMO simulations

The annual and interannual climate over the region is characterized mainly by the monsoons and ENSO events. According to Aldrian and Susanto (2003) the region is divided into three types of climate patterns, the monsoonal, the semi-monsoonal and the anti-monsoonal type of climate. They found that the southern monsoonal climate is the most stable with the lowest year-to-year standard deviation. According to rain gauge measurements, the monsoonal pattern exhibits a precipitation maximum in May/June/July and a dry period in December/January/February, while the semi-monsoonal pattern shows two peaks, a larger one in November/December and a smaller one in March/April. The anti-monsoonal pattern has almost the opposite pattern of the monsoonal pattern. In the forthcoming analysis, we will examine the long-term rainfall variability simulated by REMO in comparison with observations. Then we will look at the improvement by using a resolution hierarchy from T106, REMO 0.5° and 1/6° resolutions and will perform some sensitivity studies. The analysis will focus on the five major islands and the three sea regions as shown in Fig. 2.

3.1 The five major islands

Figure 3 illustrates the results of REMO simulations with three different lateral boundaries over five major islands. Java is a unique island with a homogenous strong monsoonal pattern, while the others have mixed patterns between monsoonal, semi-monsoonal and anti-monsoonal. REMO-ERA produces Java's rainfall pattern quite well. However, REMO-ERA sometimes overestimates the peak of the wet season rainfall and produces a longer dry period with underestimated rainfall amounts. REMO-NRA overestimates the wet season and REMO-ECHAM does not show a good contrast between the wet and the dry seasons. From a previous analysis with the ERA15 data Aldrian et al. (2003), the dry monsoon region has a larger spatial extent covering most of Sumatra, which indicates a drier Java or longer dry period for Java. In the analysis with ECHAM4 data, the spatial extent of the wet semi-monsoonal region reaches Java Island and indicates a longer wet season for Java. The analyses of the rain gauge Aldrian et al. (2003) shows that the border between the dry and wet regions lies in the third portion of southern Sumatra. REMO is a hydrostatic climate model, which suffers from errors due to weak vertical movements near steep orography. Under dry conditions, the limitation is even worse, when the supply of water vapor is lacking and the remaining convection is initiated from the orographic uplifting. The orographic convection is barely present in REMO because the 0.5° grid system does not resolve the orography well. A similar finding with a 1° grid RCM for the Indian monsoon region has been reported by Bhowmik and Prasad (2001). Thus, there are large discrepancies

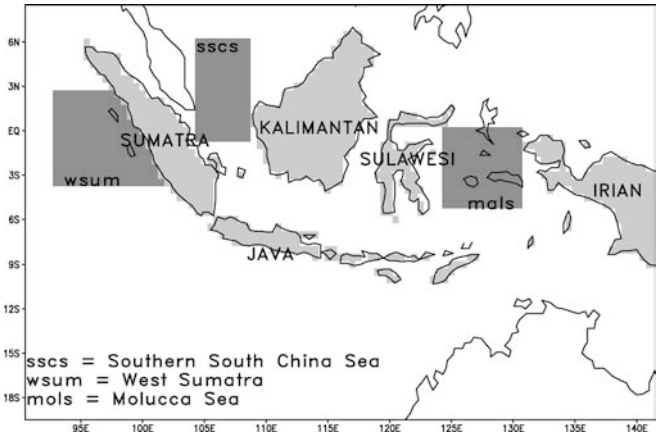

Fig. 2 The five major islands and three sea areas examined in this study

between observations and REMO, when REMO-ERA underestimates rainfall in the dry period. Over the other islands, the problem does not appear as strong as over Java because the contrast between dry and wet season is not so strong. During two ENSO events in 1982 and 1991 (the later not shown in Fig. 3), the variability of the

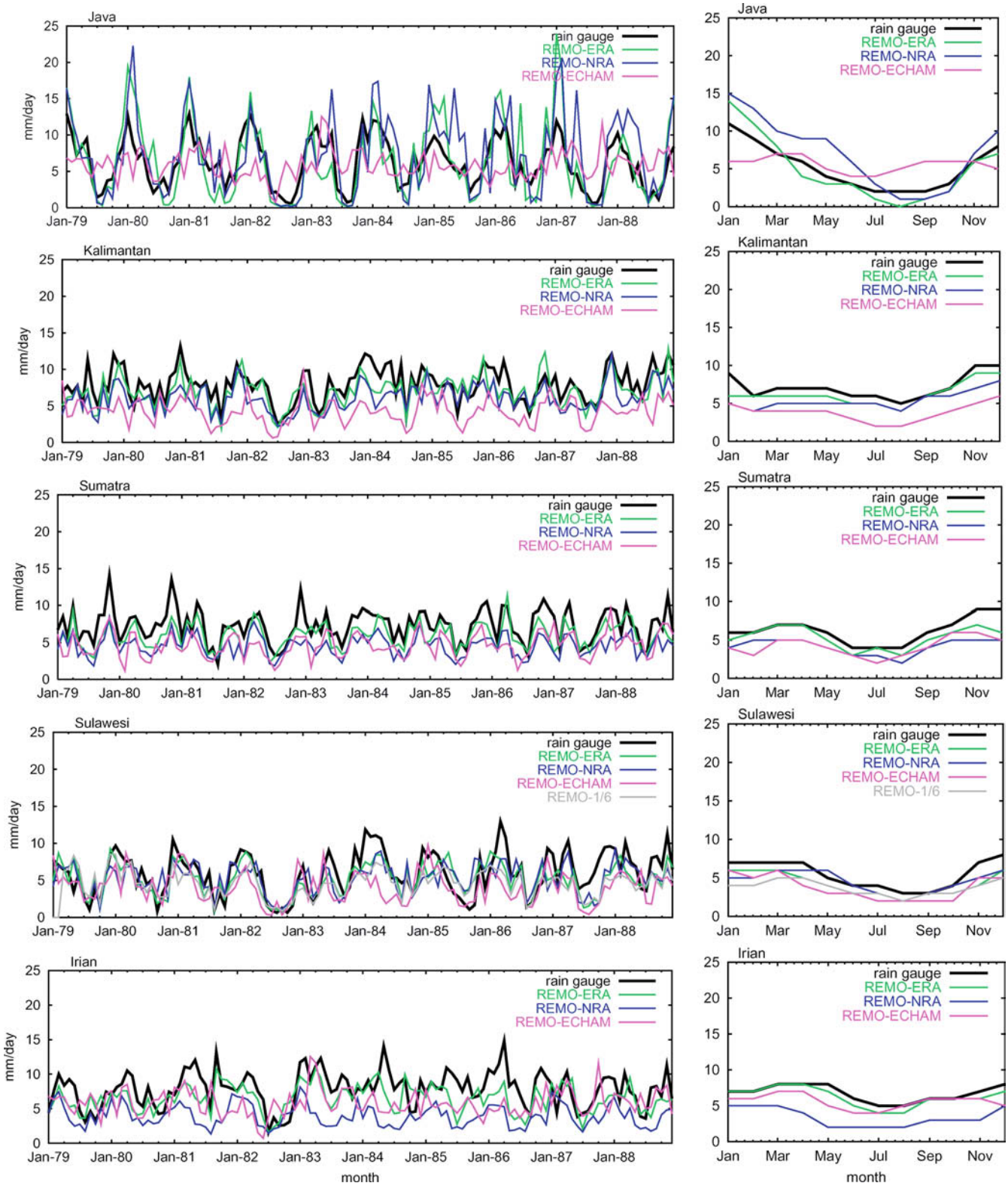

Fig. 3 Weighted area averages of the variability of simulated and observed rainfall for the five major islands (*left*) and their corresponding monthly means (*right*). For clarity, only the first 10 year variabilities are shown

reanalyses-driven REMO simulations agrees with observations. Even REMO-ECHAM4, which usually shows an overestimated dry period, has a significant fall at the beginning of the dry period.

Over the other islands, REMO simulations mostly underestimate the amount of rain. For most simulations (with the exception of REMO-ECHAM over Java) agreement with observations is good. The quality of the simulated variability of REMO-ERA15 decreases from Java to Kalimantan, Sumatra, Sulawesi and Irian. During the strong El Niño year of 1982 the variability of the model results for major islands with different model boundary conditions are consistent, including REMO-1/6. The correlation between REMO-ERA and REMO-1/6 is high (0.946) in all years. The correlation values in Irian are low because the island is located at the lateral boundary zone of the RCM. The prognostic variables on the entire outer boundary of REMO are identical to the values of the corresponding driving model. The prognostics equations are only solved for the interior model grid points. Spurious precipitation values thus appear in the outermost part of the interior domain. In addition, Irian has the lowest density of rain gauges, which contributes to a poor quality of observed rainfall area averages.

REMO-ERA performances are always better than those of REMO-NRA and REMO-ECHAM, since REMO-ERA has a better monsoon representation than the others. ERA15 provides the best forcing fields among the three. NRA has originally lower resolution than ERA15, no specific humidity in the upper nine levels and no information on the liquid water content. Although having such quality, REMO-NRA could produce good simulations because we are dealing with the lower atmosphere and the NRA quality in the lower level is good. Unlike the other simulations, REMO-NRA fails to improve the representation of the local phenomena over eastern Sulawesi (Table 2).

At T106, ECHAM4 exhibits (not shown) considerably less variability over Java than the two reanalyses and the monsoons are not well simulated. However, during strong ENSO years its quality is improved. Similar characteristics appeared in the REMO-ECHAM simulation at 0.5° resolution. Furthermore, ECHAM4 has a different time accounting system, using Julian days instead of real calendar days. As monthly averages in ECHAM4 are based on 30 days (see Table 1), the different times involvef may affect accuracy. In spite of this, REMO-ECHAM produces good results over Kalimantan, Sulawesi and especially over Sumatra, and shows stronger improvements during the ENSO years of 1982 and 1991.

Table 2 Correlations between rainfall simulations in REMO and global models and observations for the five major islands

Island	REMO			Global		
	ERA	NRA	ECHAM4	ERA	NRA	ECHAM4
Java	0.798	0.716	0.173	0.815	0.691	0.533
Kalimantan	0.780	0.668	0.422	0.780	0.761	0.417
Sumatra	0.708	0.682	0.637	0.764	0.639	0.472
Sulawesi	0.645	0.577	0.541	0.450	0.680	0.506
Irian	0.434	0.350	0.143	0.399	0.443	0.223

Over Sulawesi, another REMO simulation at 1/6° resolution is also available with a correlation value to observation similar to that at 0.5°. In fact, for the last ten years, the higher resolution simulation is a reproduction of the coarser one. Thus, in comparison to the observations at the 0.5° resolution, there is not much improvement by going to a higher resolution for Sulawesi. Limited data quality at 0.5° may not be suitable for that comparison.

Despite all this, the quality of each REMO simulation is highly comparable to its original lateral boundary counterpart. A high correlation result, as shown in Table 2, corresponds to a high correlation at the GCM resolution and so do most low correlation results. Exceptions to these are the results for REMO-ERA and REMO-ECHAM over Sulawesi and REMO-ERA over Irian, where there are significant improvements in the REMO simulations. Both Sulawesi and Irian are close to the missing anti-monsoonal climate pattern over Molucca Sea. The improvements in this area will be discussed in Sect. 3.3. At 0.5°, the rest of the land correlations show merely the down-scaling implication of limited area modeling (note that all correlations are made at the 0.5° resolution). Notice further that the result of REMO-ERA over Sumatra and REMO-NRA over Borneo are degraded (Table 2). Both islands have two climatic regions (the monsoonal and semi monsoonal) and an intermediate or equatorial climate without a well-defined annual cycle as described by Aldrian and Susanto (2003). The observed weighted area averages of the whole island tend to follow the large-scale climate. Thus, long-term correlation with a GCM should produce better correlation. A better approach is to perform analyses in an area within an island and the same climatic region.

The quality of REMO simulations tends to follow the quality of the original forcing field at the coarser resolution. The quality of the REMO simulation is determined more by the quality of the boundary forcing than by the physical parametrizations. ECHAM4 at T106 is driven by AMIP2 SST, which is presumably as good as the observed SST applied in the reanalyses. However, the quality of atmospheric circulation is lower due to the free atmospheric simulations, while reanalyses are bounded, to some extent, to the assimilated synoptic data. REMO may inherit many of the systematic errors from the global model.

Beside correlation to observations, another measure of REMO performance is the mean difference between REMO simulations and observations. The mean error is useful in calculating the mean bias from a two-sided distribution and is calculated using the following formula:

$$\overline{err} = \overline{(x - x_{obs})} \tag{1}$$

Figure 4 shows the mean errors in REMO rainfall simulations for the five major islands using three different lateral boundaries and for the original simulation at the GCM resolution. From that figure, the regional model errors are sometimes opposite in sign to those of the GCM although their absolute values are still confined to the GCM ones. For the ERA-driven simulation, there are considerable improvements of correlation or reduction of errors except for some months over Java. Over Sulawesi, ERA15 has large errors in April/May/June due to the missing anti-monsoonal pattern. With NRA, notable error reduction exists over Sulawesi only. From Table 2, REMO-NRA fails to show improvements of correlations over Sulawesi, but when using mean error analysis, an improvement becomes apparent. For ECHAM4 there is no significant improvement over all five major islands. The error over Irian from the REMO-ECHAM is similar to that of ECHAM4 (that is, it follows the lateral boundary condition). The other two REMO simulations over Irian, however, do not exhibit similar features. In fact, except over Java, the mean errors over other islands by REMO-ECHAM resemble those of ECHAM4 with larger values. Similar parametrizations at both resolutions may be responsible for this feature. The mean errors over Java are the largest for the different lateral boundary forcings. This island has a strong monsoon contrast between the dry and wet periods, which REMO-ECHAM fails to simulate.

3.2 The three sea regions

The three sea regions (see Fig. 1) are West Sumatra (WSUM), the Molucca Sea (MOLS) and the southern

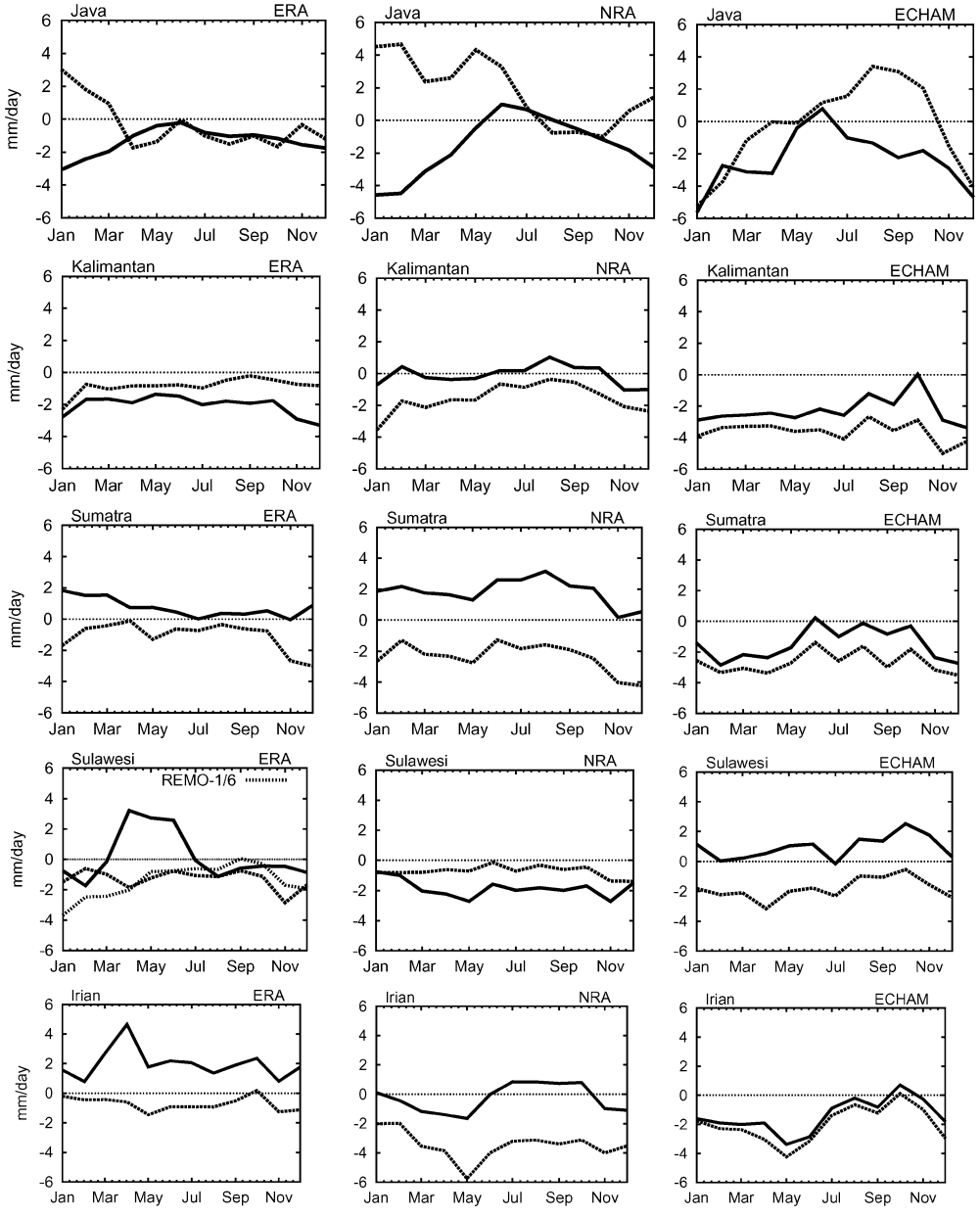

Fig. 4 Monthly mean errors of rainfall simulations (mm/day) for five major islands with three different lateral boundary forcings from ERA (*left*) NRA (*middle*) and ECHAM4 (*right*) at the GCM resolution (*solid lines*) and the REMO 0.5° resolution (*dashed lines*)

part of the South China Sea (SSCS), which represent the monsoonal, anti-monsoonal and semi-monsoonal region, respectively. The WSUM region has high average rainfall all year long. The MOLS has the anti-monsoonal type climate and is much affected by ENSO events. The SSCS has the semi-monsoonal character with double rainfall peaks in September/October/November and March/April/May. It is difficult to verify the results over the ocean because there are no observed ocean rainfall data with comparable resolution in this region and the precipitation climatology tends to lack observations over the oceans and should be treated with caution. Here, we use the secondary ocean data from GPCP. Before looking at the rainfall variability, we will discuss the quality of the SST data used by REMO.

Table 3 summarizes the quality of the SST data sets from the three lateral boundary fields in comparison to an independent GISST2.3 data set through the root mean square error (RMSE). The RMSE is useful in calculating the absolute mean error regardless of the distribution type and is defined as follow:

$$RMSE = \sqrt{\overline{(x - x_{obs})^2}} \quad (2)$$

The SST in SSCS has the least error in comparison with other regions, while MOLS has the largest error, where the RMSE reaches more than 0.5 °C. Another quality measurement is the monthly mean error as shown in Fig. 5. Both reanalyses have large negative biases over MOLS, but the smallest bias in the other two regions. From both RMS and mean errors, both reanalyses have similar SST data quality since they may have been derived from the same source. For example over MOLS, the correlation value between the two SST is high (0.993) and the RMS error is very low (0.09 °C). Over SSCS, agreements among SST are high, except for ECHAM in DJF.

The results of the three REMO simulations over sea are shown in Fig. 6. As in the case of the simulations over Sulawesi, the simulations over the Molucca Sea show a significant improvement for REMO-ERA, a small improvement for REMO-ECHAM and deterioration for REMO-NRA when compared to the global driving fields. Both land (Sulawesi) and sea (Molucca) correlations decrease by 20% from the original NRA to REMO-NRA. NRA has a coarser resolution than the other two. NRA and ERA have very similar SST and both have similar negative biases in relation to the GISST2.3 SST data. However, REMO-NRA fails to show improvement over Molucca. In addition the quality of the atmospheric representation, either the resolution or lack of some parameter fields by NRA such as the liquid water content and upper air specific humidity in higher levels, contributes to this discrepancy. Interestingly, REMO-ECHAM shows a small improvement over this region, although a bias of 0.5 °C is observed between SST of ERA and ECHAM4.

With ERA15 as a lateral boundary condition, REMO generally overestimates rainfall over the ocean. However, over the SSCS where the SST has the smallest difference compared to GISST2.3 SST, REMO-ERA gives a realistic rainfall amount. Thus, in the least error prone region (SSCS), the agreement is rather high and the time series are better correlated than in the other regions. However, as shown in Table 4, these high correlations depend on the quality of the lateral boundaries. Over SSCS the quality of the rainfall variabilities of the driving fields is also high. In the case of ECHAM4, large errors in this region will cause large errors in REMO simulations as well. The situation over SSCS shows that realistic SSTs lead to high-quality rainfall simulation both at GCM and REMO resolution, underlining the importance of correct SST forcing. The occurrence of local precipitation maxima over the sea (i.e., at the grid point scale) might be linked to a feedback between local circulation (enhanced low-level convergence) and release of latent heat of condensation, producing local warming and subsequent enhanced convergence and vertical motions. This feature has been previously discussed in Giorgi (1991).

Over WSUM, REMO performance resembles the quality of the corresponding lateral boundary forcing. Moderate SST agreement and low observed rainfall

Table 3 REMO root mean square errors (°C) of SST for the three sea regions (in comparison to GISST2.2 SST)

	Southern South China Sea	Molucca Sea	West Sumatra
REMO-ERA	0.153	0.577	0.330
REMO-NRA	0.145	0.554	0.317
REMO-ECHAM	0.278	0.339	0.342

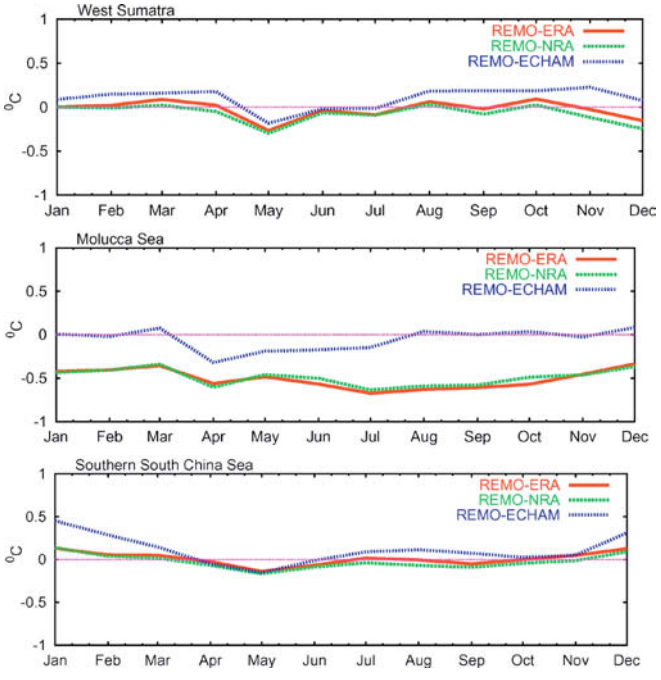

Fig. 5 Monthly mean SST errors (°C) in the three sea regions

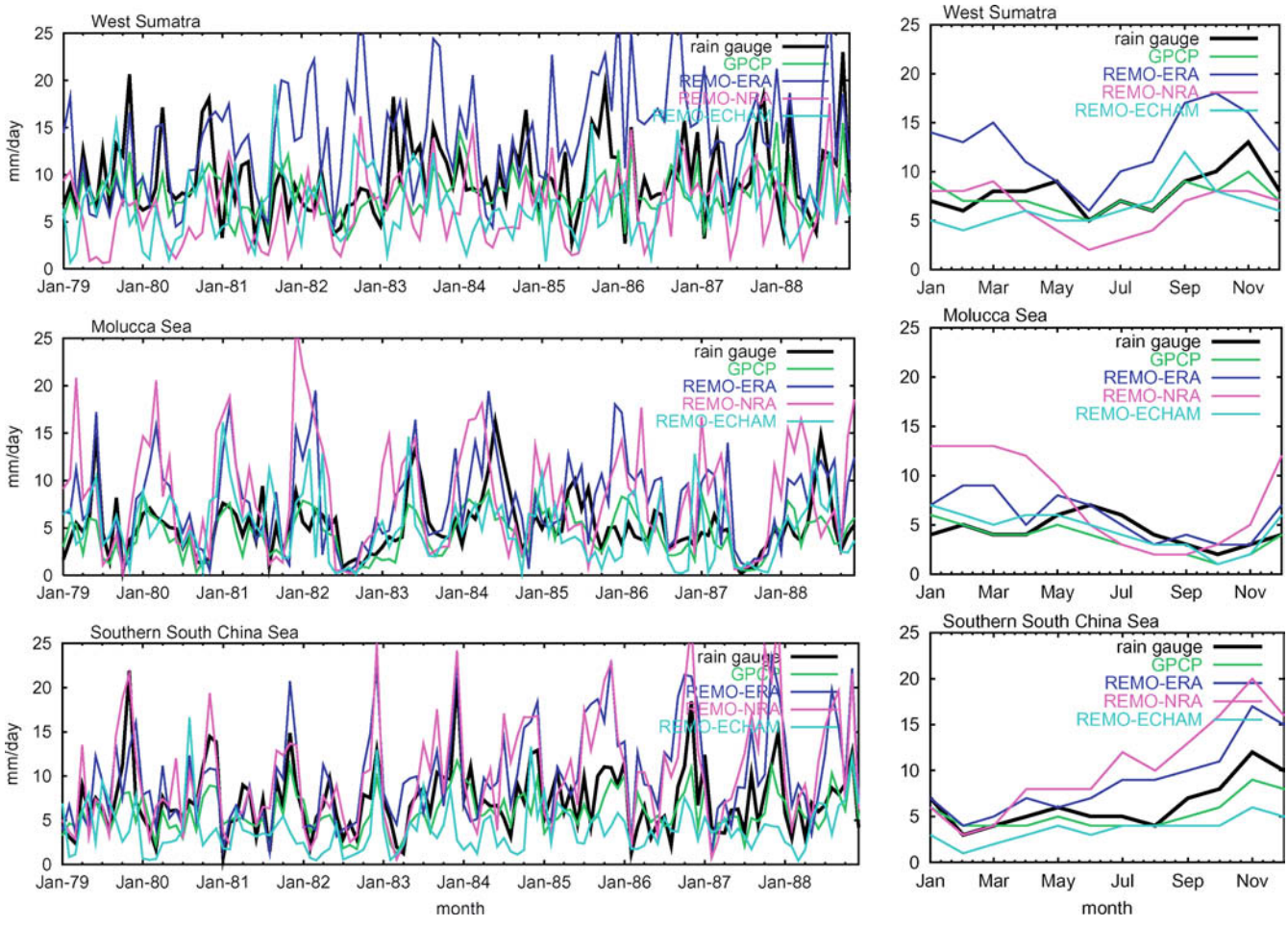

Fig. 6 As Fig. 3, but for the three sea regions

Table 4 Correlations between rainfall simulations in REMO and global models and observations for the three sea regions

Sea region	REMO			Global		
	ERA	NRA	ECHAM4	ERA	NRA	ECHAM4
West Sumatra	0.390	0.191	0.118	0.370	0.055	0.052
Molucca Sea	0.570	0.290	0.391	0.222	0.517	0.345
Southern South China Sea	0.680	0.641	0.283	0.748	0.638	0.320

quality may also be responsible for the discrepancies. Due to the lack of rainfall data over the sea, monthly mean errors such as in Fig. 4 for simulations over land cannot be performed.

3.3 Improvement through higher resolution

Figures 7 and 8 present the improvement by REMO simulation over Sulawesi in a hierarchy of model resolutions from T106 or 1.125° (bottom right) to 0.5° (bottom left) and to 1/6° (upper right) in comparison to the observed rainfall at resolution 0.5° (upper left). These examples are taken from a normal year (a non-ENSO year) and from peaks of the wet (January) and the dry season (July). Sulawesi has two climate systems (bimodal system). They are the regular monsoonal system in the south part of central and north Sulawesi Island and the anti monsoonal system in the eastern and northern part of central Sulawesi Island. The monsoonal system has an annual rainfall maximum in December/January/February, while the anti-monsoonal system reaches it in June/July/August.

During the dry season, as shown in Fig. 7, observations show maximum rainfall in the middle and eastern parts of Sulawesi. ERA15 does not show the corresponding maxima, but REMO in both resolutions shows the correct locations and magnitudes of the maxima. Similar results are also indicated for the peak of the wet season in Fig. 8, when the maximum lies over south

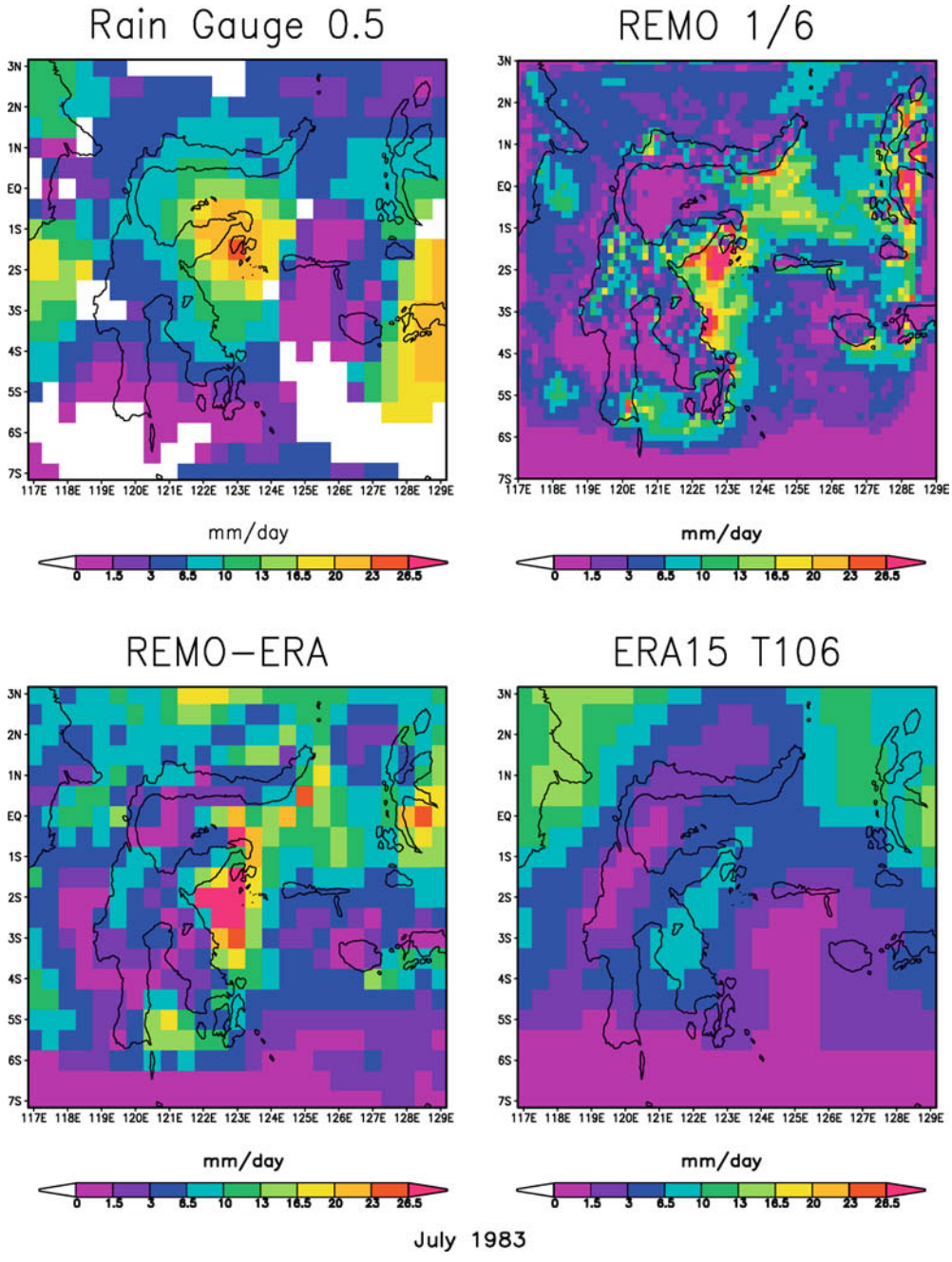

Fig. 7 An example of the effect of resolution in a hierarchy of climate models for rainfall simulation in ERA15 reanalysis, REMO-ERA at 0.5° and REMO-1/6 in comparison to observations at 0.5° resolution. The example is taken from July in a normal year 1983

Sulawesi. REMO-ERA improves the correlation with observations compared to ERA15 over Sulawesi. The improved correlation indicates a more realistic model climate in REMO for this area and reveals a formerly obscured local phenomenon.

Higher resolution (at 1/6°) also gives more vigorous orographic rainfall over Sulawesi than for coarser resolution. There is a general tendency of RCMs to overpredict precipitation amounts over high topography (see Mc Gregor 1997 for a review), presumably because of incorrect handling of the gradients along steep sigma surfaces. Similar findings have been reported by Menendez et al. (2001) and Nobre et al. (2001) over South America and Mc Gregor and Walsh (1994) over Australia.

The representation of the anti-monsoonal climate over the Moluccan archipelago is not as good as that for eastern Sulawesi because the Moluccan archipelago is close to the boundary of the REMO-1/6 domain. If it were extended farther east at high resolution, we would expect a better representation of the anti-monsoonal system. A remaining deficiency is the common problem of overestimated rainfall over the ocean at both REMO resolutions.

In summary, the downscaling by REMO with three spatial resolutions shows a better rainfall representation over the Molucca region and part of Sulawesi. The anti-monsoonal system was missing in the T106 analysis. Although, the boundary forcing does not contain it,

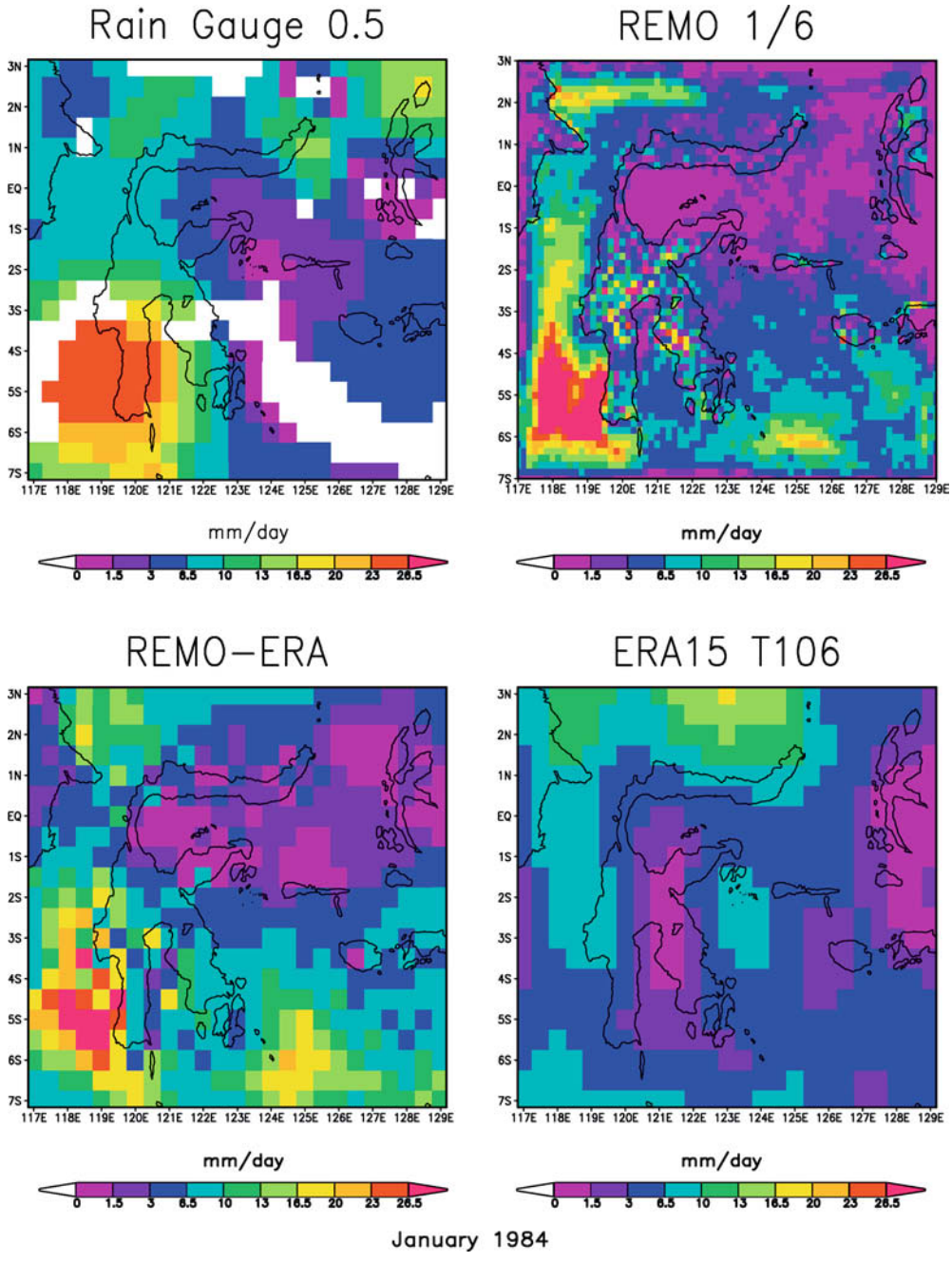

Fig. 8 As Fig. 7, but for January 1984

REMO could produce this bimodal system at higher spatial resolution, indicating that the anti-monsoonal circulation over Molucca and east of central Sulawesi is a local phenomenon, which cannot be resolved with a low-resolution global model at T106.

3.4 Sensitivity studies

REMO overestimates rainfall over the ocean. Although the area averages are comparable, peak values over the ocean are too high. In order to understand the possible background of this overestimation, we adjusted some parameters, which eventually would reduce the precipitation over the ocean with minimal changes over land. In doing so, we changed the minimum cloud thickness over land (ZL) and ocean (ZO), the minimum humidity level for the condensation to start (ZRTC) and of the large-scale cloud system (ZRTL), the SST and the Charnock constant (CCHAR; Deutscher-Wetterdienst 1995). The sensitivity study was performed with REMO-ERA, which shows the best results so far. The REMO-ERA with changed parameters was rerun for the first four years between 1979–1982 to allow all simulations to use the same starting point and to compare the results to the control run. Figure 9 illustrates two examples from the

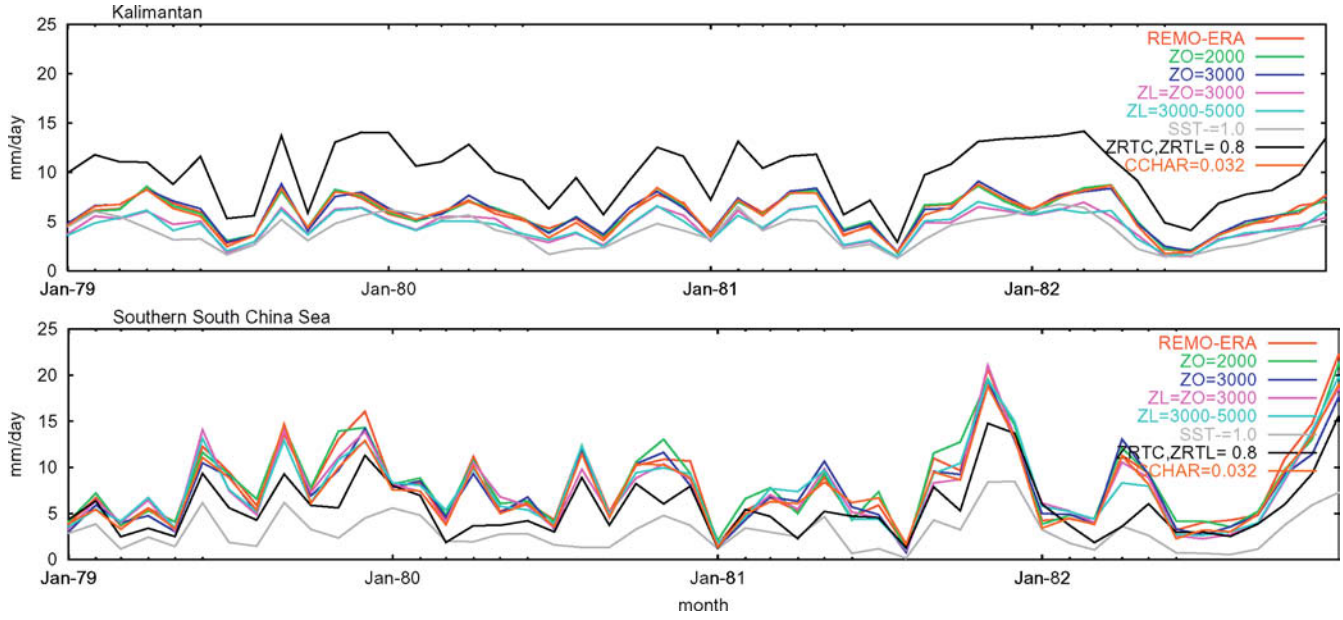

Fig. 9 Two examples of the results from the sensitivity study over Kalimantan and the southern South China Sea

sensitivity study over Kalimantan and southern South China Sea in comparison to REMO-ERA and the control run.

The minimum cloud thickness for the start of the precipitation process over land (ZL) and over sea (ZO) are set to 1500 m in REMO, but in the original ECHAM4 parametrization they ranged from 3000 to 5000 m. We changed them to 2000 m or 3000 m, or varied them between 3000 m and 5000 m and looked for effects upon rainfall over land and sea. The result shows no significant influence on rainfall over the sea. Over land, however, a reduction of the average rainfall by 1.28 mm/day over Kalimantan occurs when adopting a flexible threshold between 3000 and 5000 m.

The second approach was to apply a constant SST reduction of 1.0 °C. According to Aldrian and Susanto (2003), a lower rainfall amount is usually associated with low local SST. In order to reduce overestimation over the sea, we chose reductions of the local SST. This reduction lowered rainfall over land and sea. However, the reduction over land was less than over sea and the latter is unrealistically large (5 mm/day). This kind of sensitivity study shows the importance of SST for climate modeling over the region. Furthermore, with only a little more than 21% of land area and a widespread scatter of small islands, the mean climate of the region is oceanic or ocean affected.

Another sensitivity test is to change the minimum relative humidity threshold for the condensation to start in a grid volume. This parameter involves two precipitation processes, the convective and large-scale precipitation. In the original formulation, both parameters (ZRTC and ZRTL) were set to 60%. Changing them to 80% causes significant changes over land and sea. Interestingly, the rainfall over land increases somewhat, while the rainfall over sea decreases significantly.

Evaporation is a key process for the atmospheric water cycle and thus precipitation processes. The Charnock constant is a measure for the evaporation rate or the evaporation flux into the atmosphere from the ocean. In the original ECHAM4 parametrization, this parameter is set to 0.032. REMO also uses this value but only for a grid cell size above 0.5°, while for finer resolution a value of 0.0123 is used. In this sensitivity study, the original ECHAM4 parametrization is used. The result shows only a slight precipitation decrease between the sensitivity and the control run. As in the case of changing SST, the decrease of rainfall over the sea is a little larger than that over land. This fact marks this constant as the next good candidate to solve the problem of rainfall overestimation over sea areas.

Table 5 summarizes the seven sensitivity studies. From the analysis described, there are three possible candidates to solve the problem of rain overestimation over the sea. These are the reduction of SST, changed ZRTC and ZRTL, and a changed Charnock constant. Drastic reduction takes place when the REMO SST is reduced by 1.0 °C and ZRTC and ZRTL are set to 80%. However this reduction takes place also over land, while the intention is to have reductions over sea only. Furthermore, when we compare the result with observations, this reduction does not always result in the rainfall amount being close to observations. It may be a combination of several possibilities, already discussed, that are responsible for the discrepancies of rainfall between REMO and observations. From the three sea regions, the least error-prone region (SSCS) has the least bias. In conclusion, the combination of prescribed SST and parametrization errors may be key contributors and a coupled ocean atmospheric model is needed for further investigation.

Table 5 Mean difference (mm/day) between sensitivity studies and control run (REMO-ERA)

Sensitivity type	Land					Sea		
	Java	Kalimantan	Sumatra	Sulawesi	Irian	Wsum	Mols	SSCS
ZO = 2000	0.003	0.034	–0.018	0.051	0.078	–0.092	0.037	0.178
ZO = 3000	0.413	0.114	0.678	0.508	0.443	–1.241	–0.224	–0.569
ZL,ZO = 3000	–0.471	–1.243	–0.757	–0.857	–0.617	–1.093	–0.659	–0.568
3000 < (ZL,ZO) < 5000	–0.460	–1.289	–0.781	–0.831	–0.583	–1.049	–0.415	–0.497
SST = SST–1.0	–1.782	–1.788	–1.634	–2.266	–0.789	–4.657	–4.866	–5.068
ZRTC, ZRTL = 80%	2.569	4.135	5.675	2.655	3.888	–1.336	–3.307	–2.459
CCHAR = 0.032	–0.046	–0.057	–0.014	–0.191	0.148	–0.351	–0.425	–0.673

4 Predictability of rainfall simulated by REMO

Lorenz (1969) found that each scale of motion possesses an intrinsic finite range of predictability. A small error in the initial state of a nonlinear system will grow and will render a forecast useless after some time, regardless of the model error. For this study we performed ensemble simulations by changing initial land and atmospheric states to measure the internal variability of the model. Ji and Vernekar (1997) applied a similar technique for a RCM, but for a shorter term. The simulation was set up by varying the initial condition by 12 h from 0 to 72 h and making a control run at 0 h and six ensemble members. With this setup, we changed all lateral boundaries at the initial condition and the exact length of the first month of simulation will be slightly different among ensemble members. There are two ensemble simulations using boundary forcings from ERA15 and ECHAM4 to represent reanalyses and GCM model simulations. This predictability study refers to the predictability of the initial condition or the predictability of the first kind. We will analyze how strong the initial condition affects the short and long-term simulation.

From long-term simulations with ERA15 and ECAHM4 with lateral boundary forcings as shown in Fig. 10, there are only small internal variabilities among the control run and other ensemble members. All ensemble members follow strongly the variability prescribed by the control run. This characteristic appears in all seasons and regions (not shown). The variability of ensemble members follows the control run right after the first month. Thus, after a while, there is no effect left from changing the initial condition or, in other words, the boundary condition strongly controls the variability of each ensemble member. In comparison to land, the variability over sea is larger in both types of REMO experiments. The internal variability does not grow or decay with time but establishes itself as an intrinsic finite range of REMO predictability.

4.1 Intrinsic errors

A more cautious investigation employs monthly root mean square errors (RMSE) of the internal variability. By looking at this, we exclude other external errors and examine solely the intrinsic climatological error due to different initial conditions, since we maintain similar model parameters and lateral boundaries. Any errors will be due to the initial condition as a possible source of errors in REMO simulations. The intrinsic climatological error over the five major islands and the three sea regions are shown in Figs. 11 and 12.

Interestingly, each island has a unique and coherent annual pattern. Java has the largest error especially using REMO-ERA, whose RMSE reaches almost 3 mm/day in April. This RMSE is significantly large considering the average value of REMO-ERA and REMO-NRA in April of 4.87 and 9.20 mm/day respectively. Other islands have less than a third of Java's error. From both types of REMO experiments, there are considerably larger errors during Northern Hemisphere spring (March/April/May) than during other seasons. Indonesia experiences the transition between the wet and the dry monsoon periods at this time of the year. On the other hand, there is also a systematic pattern of the lowest error during the Northern Hemisphere summer (June/July/August), when most of Indonesia experiences the peak of the dry period. Furthermore, this lowest error period is the most coherent period. Thus we expect that simulations of rainfall over Indonesia have the highest predictability at this time of the year. In other words, this season is the best period to examine other predictabilities beside internal predictability due to initial conditions. The other two seasons (December/January/February and September/October/November) have errors in between the two seasons discussed earlier.

Over sea areas, the variability of the intrinsic climatological error due to initial condition is less coherent and has magnitudes higher than those over land. Moreover, there is no common pattern as over the major island areas. The highest spring and lowest summer errors are detected over the Molucca Sea. REMO simulations often produce overestimations of rainfall over the sea. The internal climatological error is also responsible for such discrepancies. Thus, from the result of this predictability study alone, higher error over the sea is expected from REMO simulations over Indonesia.

Consistent and large intrinsic errors in spring for a large part of Indonesia contribute to lower predictability skill in this season and may be related to the spring predictability barrier. The spring predictability barrier

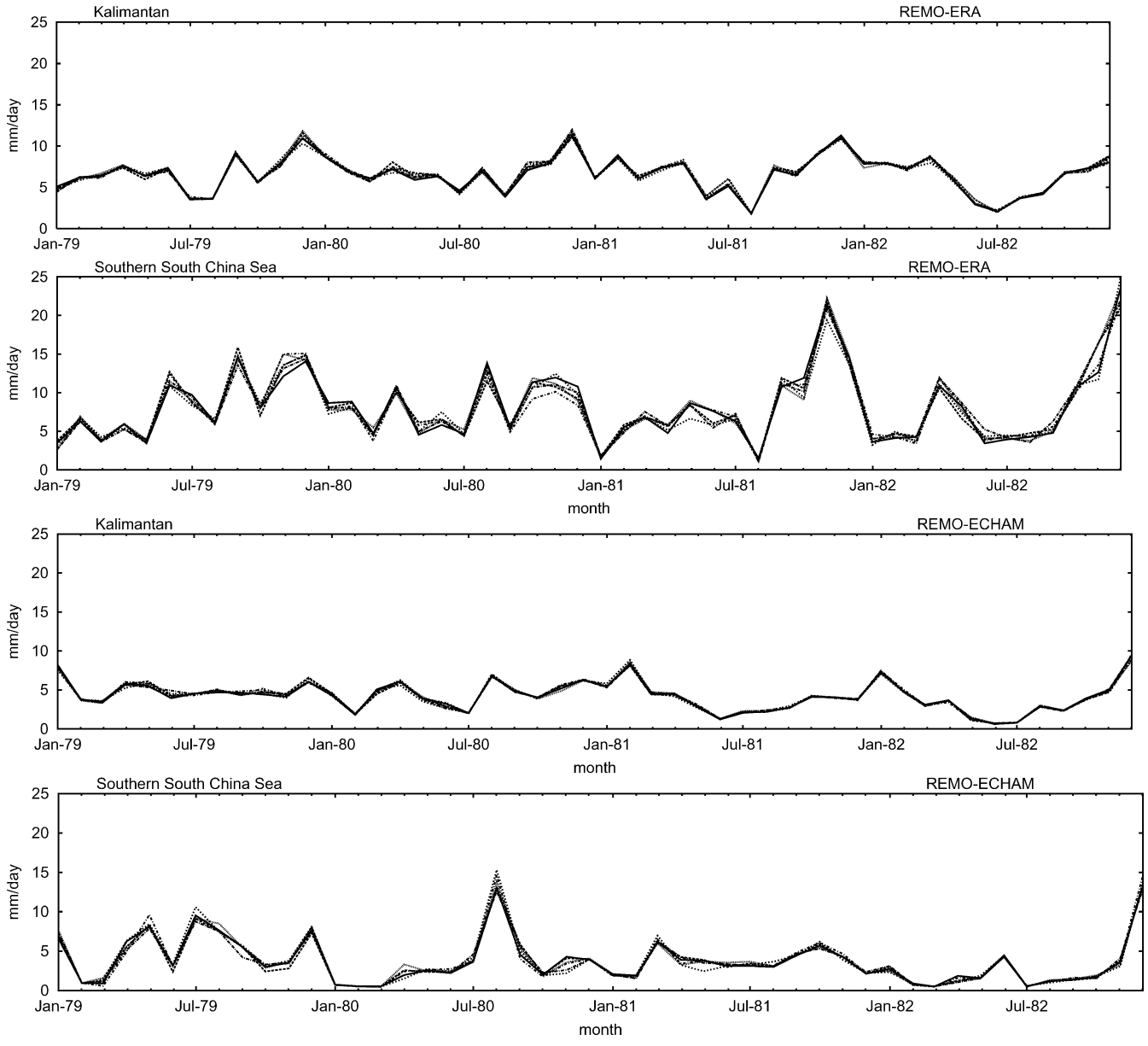

Fig. 10 Examples of the results from the long term predictability study over Kalimantan and the southern South China Sea from REMO-ERA and REMO-ECHAM. Each graph consists of a control run and six ensemble member simulations. For clarity only the first four years are shown

refers to a lower skill generally observed for predictions that extend through boreal spring (Blumenthal 1991; Goswami and Shukla 2000; Latif and Flügel 1991; Latif and Graham 1992; Webster and Yang 1992; Balmaseda et al. 1995; Davey et al. 1996; Moore and Kleeman 1996; Chen and van den Dool 1997; Yu et al. 1997; Flügel and Chang 1998; Latif et al. 1998; Weiss and Weiss 1999; Goddard et al. 2000; Thompson and Battisti 2001).

The predictability study suggests a monthly or seasonal variability of the intrinsic RMSE error of REMO over Indonesia. It has been demonstrated previously (e.g., Errico and Baumhefner 1987; Vukicevic and Errico 1990; Paegle et al. 1997; Laprise et al. 2000) that the predictability of regional climate models is distinct from that of global models. The RMSE among ensemble members, in contrast to global models, approaches a value much smaller than the variance due to natural variability. While those studies concentrated mainly on variables such as geopotential, temperature or wind field, the present study examines the rainfall. In this study the values of RMSE of rainfall among ensemble members do not produce a single value asymptote, but rather follow the intrinsic natural variability, which varies by region and season.

Analysis previously showed a possibility that a local phenomenon, such as in Molucca, could appear in a regional simulation that has no counterpart in the original simulation at T106. This local phenomenon ap-

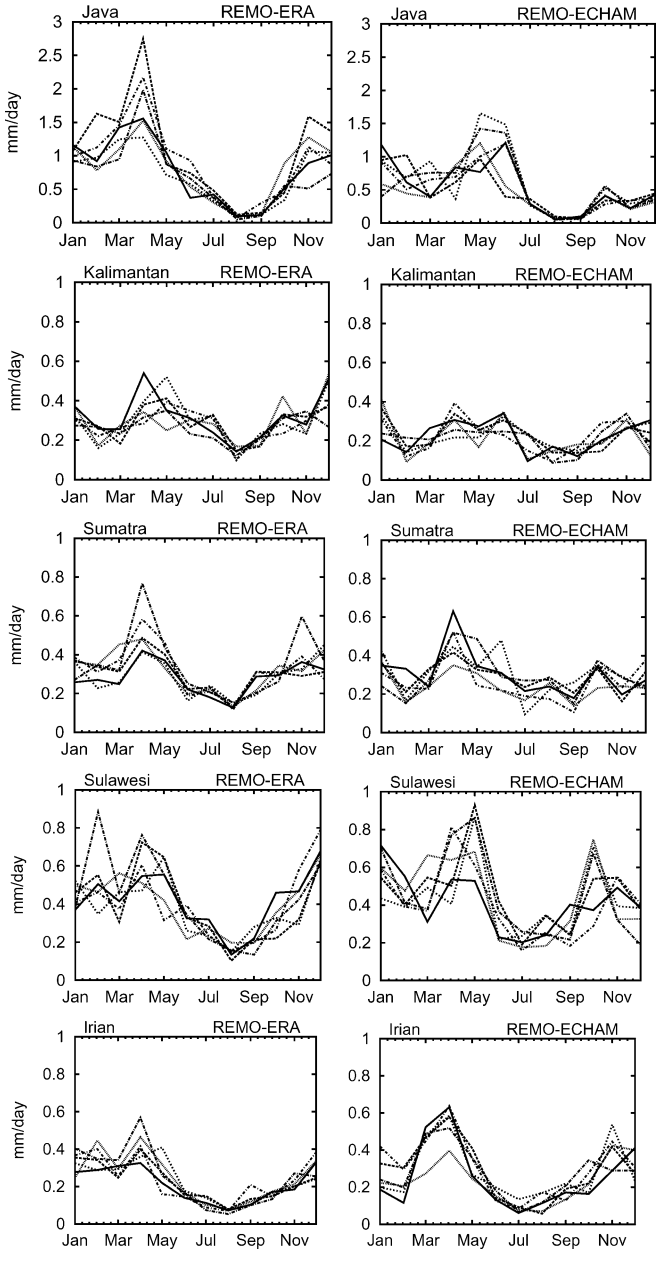

Fig. 11 Monthly root mean square difference (mm/day) of ensemble members to control run for five major islands as a measure of the internal predictability of six ensemble members caused by the initial values. Note that Java has magnitudes three time larger than the other islands

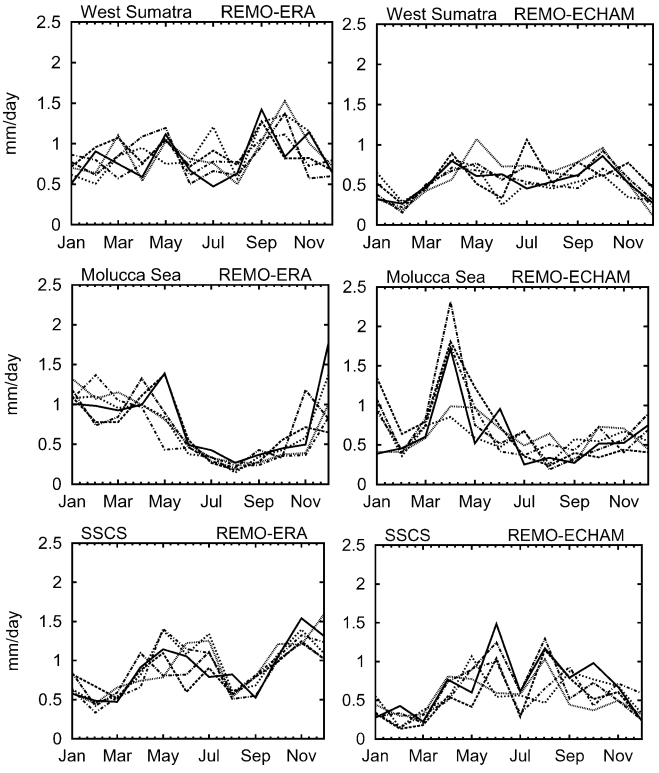

Fig. 12 As Fig. 11, but for three sea regions

pears in all ensemble members (not shown) with a high predictability or low internal variability as in other areas. Thus REMO enhances the "just in time" local phenomenon independent of errors caused by different initial conditions. This characteristic is very important and useful for some REMO applications. For example, the regional model simulation can be used in a future climate scenario as a down-scaling tool. It is not necessary to run the climate simulation for a longer period. We may proceed directly to the intended period without having to worry about the initial conditions. This is only true for local convective phenomena or in a small land area such as the maritime continent, otherwise we need to wait until the soil reaches its equilibrium and restart the simulation using that equilibrium soil.

The lateral boundary condition, which is updated every 6 h, is responsible for the high predictability level. REMO cannot keep the memory of an initial condition after some consecutive changes of the lateral boundaries, which eventually limits the degrees of freedom of REMO. There are ways to increase the degrees of freedom in REMO simulations. For example, we could supply SST from a different time period for each ensemble member. This kind of study would refer to the second kind of predictability (boundary value problem). Another possibility is to supply the ocean surface boundary condition from a stand-alone ocean simulation and couple that with REMO. Rather than changing the initial condition once, the ocean model could supply different SST information every 6 h and hence give more degrees of freedom to REMO.

The result indicates that REMO has a small internal variability, which shows that the corresponding simulations are strongly constrained by lateral boundary conditions. An RCM should be sufficiently free to develop internal mesoscale processes in order to be useful for sensitivity studies. In this study REMO has shown its ability to enhance regional features over Sulawesi and the Molucca Sea. The strong boundary influence may also be due to the small domain size used in this study. Jones et al. (1995) concluded that the regional climate

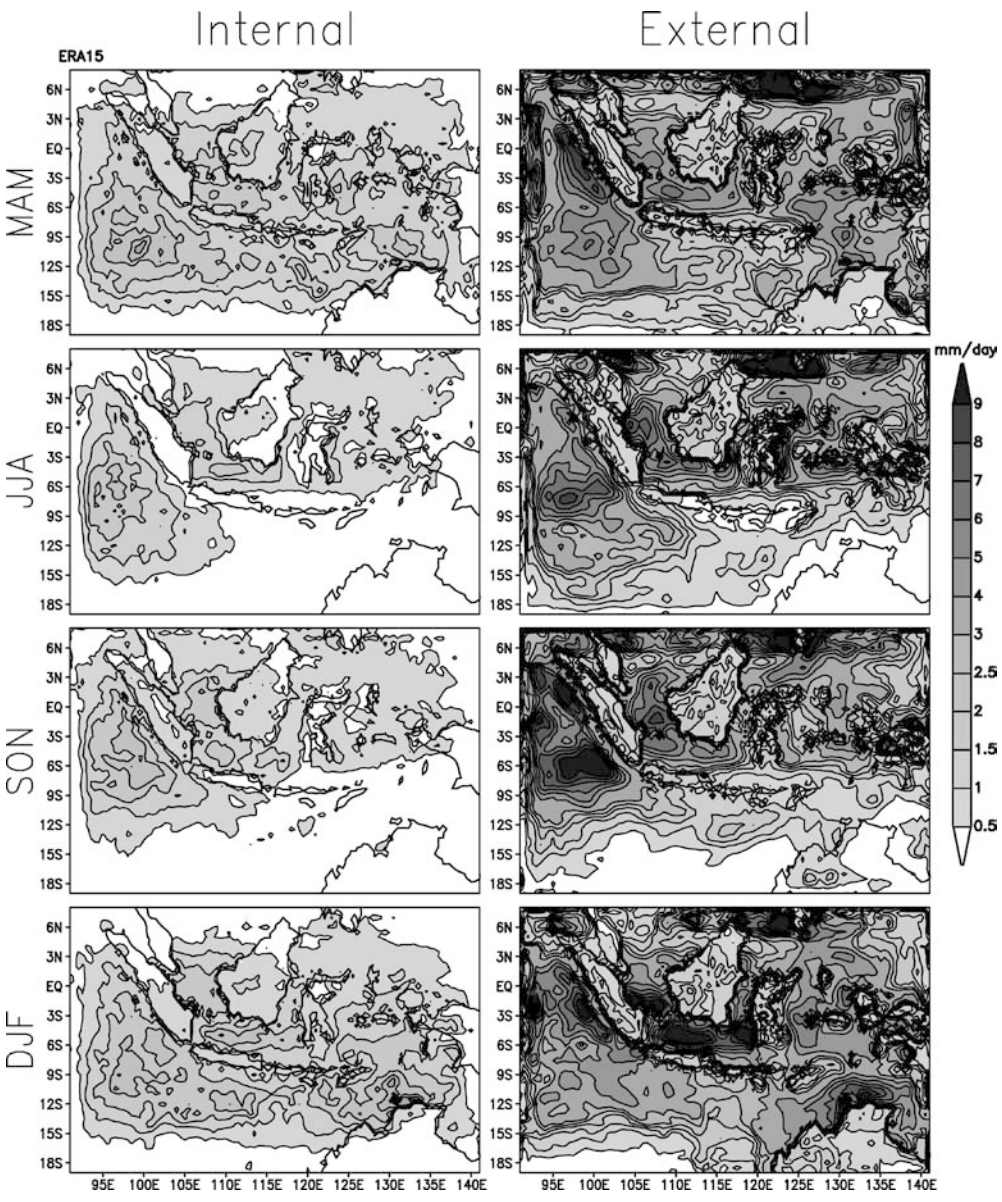

Fig. 13 The internal and external variances of the ensemble REMO-ERA simulation

model domain should be sufficiently small so that the synoptic circulation does not depart far from that of the driving GCM. However, Podzun et al. (1995) found that the domain should also be sufficiently large to allow development in the regional climate model of features having a finer scale than those skillfully resolved by the GCM. Furthermore, Bhaskaran et al. (1996) found that the tropical monsoon simulation with a RCM is relatively insensitive to model domain size, which contrasts strongly with simulation results from Europe by Jones et al. (1995).

4.2 Internal and external variances

Another measure of the predictability of an ensemble simulation is the internal and external variances or variability. The predictability is determined by the summation of those variances. In this study the internal variance is defined as

$$\mathrm{var}(x_i\langle x\rangle) = \overline{\left\langle (x_i - \langle x\rangle)^2 \right\rangle} \ , \tag{3}$$

and the external variance as

$$\mathrm{var}(\langle x\rangle) = \overline{(\langle x\rangle - \overline{\langle x\rangle})^2} \ , \tag{4}$$

where x_i is the i-th ensemble member, the $\langle x\rangle$operator denotes the ensemble average and the $\bar{x}$operator denotes the time average. The method employed here is comparable to the analysis of variance (ANOVA) method. The internal variance measures the degree of freedom of a domain and measures how high the quality with one simulation (without ensemble) will be. In this case low internal variability indicates an expected good performance by just a single simulation. Low degree of

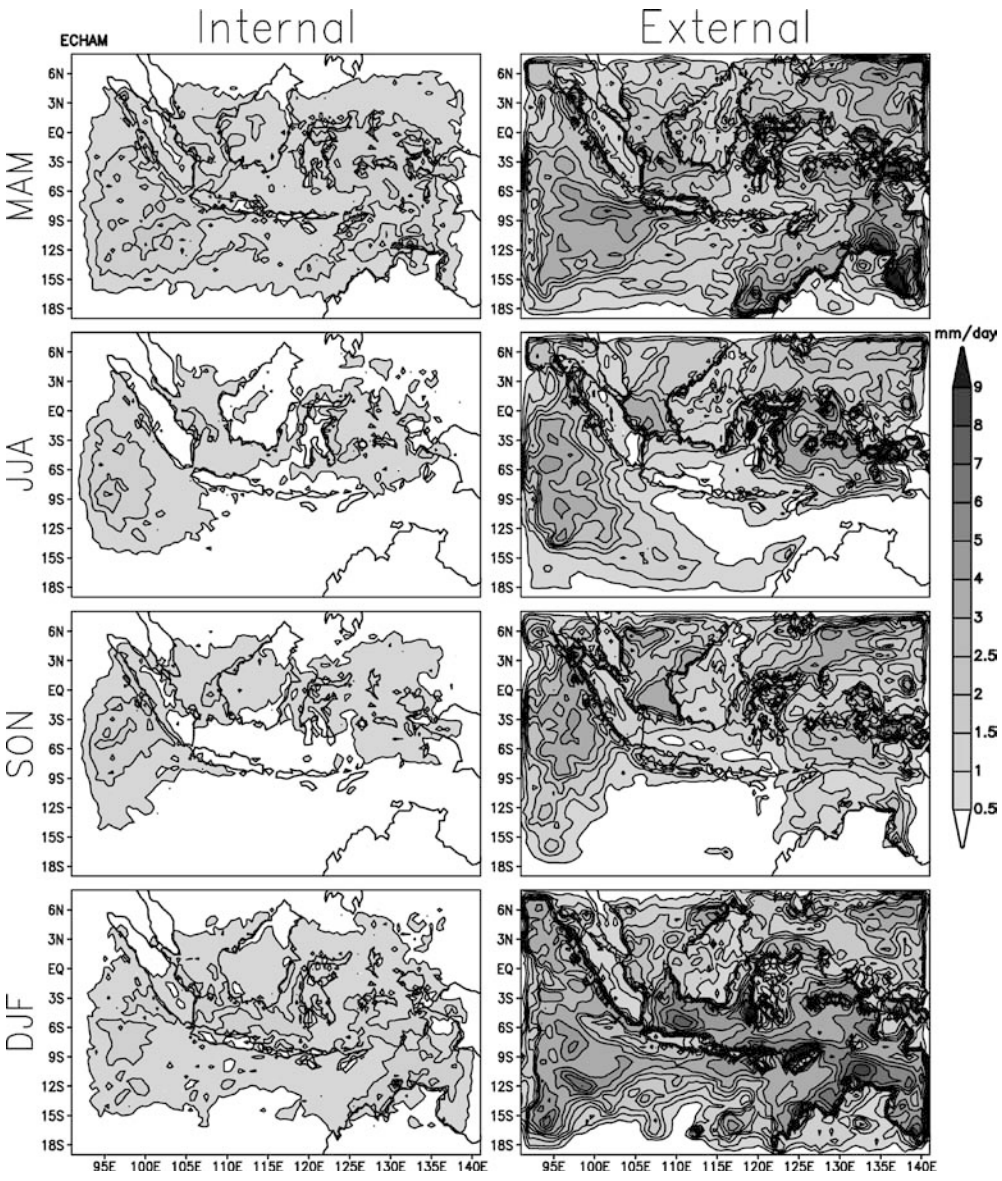

Fig. 14 As Fig. 13, but for REMO-ECHAM

freedom may also mean too strong boundary condition control, while, the external variance measures the contribution of large-scale phenomena surrounding the domain. Hence the predictability is high when the external variance is low.

Figures 13 and 14 show the seasonal internal and external variances of ensemble simulations from REMO-ERA and REMO-ECHAM, respectively. From both figures, the seasonal internal variances are only about a quarter of the external variances. Thus, variability among ensemble members is mainly due to external climate phenomena. Low internal variability may also be due to too strong lateral boundaries. The lateral boundary extends up to eight grid cells as shown in internal variances on both figures. Within the inner region, the model is capable of developing variability independent on lateral boundaries. The inner region shows variances according to climate activity, whereby higher variances exist in wetter regions or areas with higher precipitation activity. Consequently, the internal variance has a seasonal dependency according to wet and dry seasons, when JJA and SON have less variance than the other seasons. The latter condition is also true for the external condition, where higher variances are related to major seasonal disturbances in the region, such as high precipitation in west of Sumatra in all seasons, tropical storm tracks near Mindanao (not clear in REMO-ECHAM), tropical disturbances in northern Australia in DJF, and a high precipitation area over the Java Sea. Another persistent contrast exists between variances over land and sea with variances over land (or higher predictability over land) than over the sea. The persistence is highest west of Sumatra, which has high precipitation all year long or very little seasonal dependence.

Although the measure of variance presented here is able to show sources of discrepancies among ensemble members, this variance measurement is limited to

REMO only. There is a need for more ensemble quality simulations from other regional models operating in the area to determine the real quality of REMO simulation. The only comparison made here is between two different lateral boundary conditions ERA15 and ECHAM4, where the ECHAM4 boundary conditions give lower variances than ERA15. Hence, the quality of a single simulation by REMO-ECHAM is closer to its ensemble mean than for REMO-ERA. The present study shows that high predictability is achievable over land in JJA followed by SON, which is consistent with the findings in the previous subsection.

5 Concluding remarks

We have described the performance of rainfall simulations over Indonesia with REMO, driven by three lateral boundary conditions derived from two reanalyses and a T106 ECHAM4 simulation, at two different horizontal resolutions. We analyzed the results for the five major islands and three selected sea regions in the maritime continent. In addition, sensitivity and REMO predictability studies for different initial condition have been performed. The analysis focuses on monthly, seasonal and interannual variability of rainfall simulations as well as the annual cycle.

The model, in general, is able to reproduce the spatial pattern of monthly and seasonal rainfall. It produces correct variability for ENSO years but fails to show a good monsoon contrast. The simulations over land are better in this respect than over sea areas. The high quality of REMO simulations over land is due to resolved orography, while over the ocean REMO suffers from surface fluxes problems and overestimates the rainfall. The model's dependence on various sub-grid parametrizations is a very complex issue and is not fully understood at present. Analyses of a sensitivity study to reduce too strong precipitation over sea still leave some uncertainties. Beside the lateral atmospheric boundary, SST is the major factor determining the quality of simulations where the least error prone region (SSCS) has the least bias.

The results suggest the important role of lateral boundary conditions. REMO-ERA, which has the best lateral boundary fields supplied by ERA15, produces the closest simulation to observations except over Java. Despite the strong influence of the lateral boundary, REMO shows realistic improvement of a local climate phenomenon over Molucca through higher correlation (REMO-ERA and REMO-ECHAM) and mean errors (REMO-NRA).

Improvement with higher resolution is obvious from T106 to 0.5° but not to 1/6°. There is no need to go to the higher resolution of 1/6°, where there are more vigorous orographic rainfalls over Sulawesi Island. However, this should be investigated later with higher quality rainfall data. It may be that the parametrization we are using over this region is most suitable for the 0.5° resolution. Moreover, RCM parametrization schemes are normally tuned to the GCM resolution (Nouger et al. 1998). For this island, it might be necessary to use a non-hydrostatic model. Steep orography as well as the temperature gradients associated with the strong orographic convection can only be adequately simulated with non-hydrostatic models.

The predictability study shows small internal variability among ensemble members. This means that the model can be used in any place in time without worrying too much about the spin up. However, the intrinsic climatological errors as shown in the predictability analysis are worth considering. Those intrinsic errors have monthly, seasonal and regional dependences, and the one over Java is significantly large. The intrinsic error study suggests the presence of the spring predictability barrier and a high level of predictability in summer.

Acknowledgements The first author was awarded a DAAD scholarship A/99/09410. We thank Prof. Hartmut Graßl who reviewed an early version of the manuscript and supervised the study. Special thanks go to Tien Sribimawati, her group and BMG (Indonesian Bureau of Meteorology and Geophysics) for providing some rainfall data. Calculations were performed at the Deutsches Klimarechenzentrum (DKRZ), Germany.

References

Aldrian E, Susanto RD (2003) Identification of three dominant rainfall regions within Indonesia and their relationship to sea surface temperature. Int J Climatol 23: 1435–1452

Aldrian E, Dümenil-Gates L, Widodo FH (2003) Variability of Indonesian rainfall and the influence of ENSO and resolution in ECHAM4 simulations and in the reanalyses. MPI Rep 346 available from Max Planck-Institut für Meteorologie, Bundesstr. 55, D-20146, Hamburg, Germany, pp 30

Balmaseda MA, Davey MK, Anderson DLT (1995) Decadal and seasonal dependence of ENSO prediction skill. J Clim 8: 2705–2715

Bhaskaran B, Jones RG, Murphy JM, Noguer M (1996) Simulations of the Indian summer monsoon using a nested regional climate model: domain size experiments. Clim Dyn 12: 573–587

Bhowmik SKR, Prasad K (2001) Some characteristics of limited-area model-prescription forecast of Indian monsoon and evaluation of associated flow features. Meteorol Atmos Phys 76: 223–236

Blumenthal MB (1991) Predictability of a coupled ocean-atmosphere model. J Clim 4: 766–784

Bougeault P (1983) A non-reflective upper boundary condition for limited-height hydrostatic models. Mon Weather Rev 111: 420–429

Chen WY, van den Dool HM (1997) Atmospheric predictability of seasonal, annual and decadal climate means and the role of the ENSO cycle: a model study. J Clim 10: 1236–1254

Davey MK, Anderson DLT, Lawrence S (1996) A simulation of variability in ENSO forecast skill. J Clim 9: 240–246

Davies HC (1976) A lateral boundary formulation for multi-level prediction models. Q J R Meteorol Soc 102: 405–418

Deutscher-Wetterdienst (1995) Dokumentation des EM/DM Systems with contributions from Edelmann W, Majewski D, Schättler U, Prohl P, Heise E, Doms G, Ritter B, Link A, Gertz M, Hanisch T, Fischer E. Zentralamt, Abteilung Forschung, Postfach 10 04 65, 63004 Offenbach am Main, Germany

Dümenil L, Todini E (1992) A rainfall-runoff scheme for use in the Hamburg climate model. In: O'Kane JP (ed) Advance of theoretical hydrology, vol 1 (Ed.), European Geophysical Society. Series on Hydrological Sciences vol 1, Elsevier Science, Amsterdam, pp 129–157

Errico RM, Baumhefner DP (1987) Predictability experiments using a high resolution limited area model. Mon Weather Rev 115: 488–504

Flügel M, Chang P (1998) Does the predictability of ENSO depend on the seasonal cycle? J Atmos Sci 55: 3230–3243

Fouquart Y, Bonnel B (1980) Computations of solar heating of the Earth's atmosphere: A new parametrization. Beitr. Phys Atmos 53: 35–62

Gates WL (1992) AMIP: the Atmospheric Model Intercomparison Project. Bull Am Meteorol Soc 73: 1962–1970

Gates WL, Boyle JS, Covey C, Dease CG, Doutriaux CM, Drach RS, Fiorino M, Gleckler PJ, Hnilo JJ, Marlais SM, Phillips TJ, Potter GL, Santer BD, Sperber KR, Taylor KE, Williams DN (1999) An overview of the results of the Atmospheric Model Intercomparison Project (AMIP I). Bull Am Meteorol Soc 80: 29–56

Gibson JK, Kallberg P, Uppala S, Hernandez A, Nomura A, Serrano E (1997) The ECMWF Re-Analysis (ERA) 1. ERA description., ECMWF Reanalysis Project Report Series 1 ECMWF, (available from the European Centre for Medium-range Weather Forecasts, Reading, UK), pp 71

Giorgi F (1991) Sensitivity of simulated summertime precipitation over the western United States to different physics parametrizations. Mon Weather Rev 119: 2870–2888

Goddard L, Mason SJ, Zebiak SE, Ropelowski CF, Basher R, Cane MA (2000) Current approaches to seasonal to interannual climate predictions., (IRI) Tech Rep 00-01 International Research Institute pp 62

Goswami B, Shukla J (2000) Predictability of a coupled-atmosphere model. J Clim 4: 3–22

Hagemann S, Botzet M, Dümenil L, Machenhauer B (1999) Derivation of global GCM boundary conditions from 1 km land use satellite data. MPI Report 289, Max Planck-Institut für Meteorologie, Bundesstrasse 55, 20146, Hamburg, Germany pp 34

Hamada JI, Yamanaka MD, Matsumoto J, Fukao S, Winarso PA, Sribimawati T (2002) Spatial and temporal variations of the rainy season over Indonesia and their link to ENSO. J Meteorol Soc Japan 80: 285–310

Haylock M, McBride J (2001) Spatial coherence and predictability of Indonesian wet season rainfall. J Clim 14: 3882–3887

Hendon HH (2003) Indonesian rainfall variability: impacts of ENSO and local air-sea interaction. J Clim 16: 1775–1790

Huffman GJ, Adler RF, Arkin P, Chang A, Ferraro R, Gruber A, Janowiak J, McNab A, Rudolf B, Schneider U (1997) The Global Precipitation Climatology Project (GPCP) combined precipitation data set. Bull Am Meteorol Soc 78: 5–20

Jacob D (2001) A note to the simulation of the annual and interannual variability of the water budget over the Baltic Sea drainage basin. Meteorol Atmos Phys 77: 61–73

Jacob D, Podzun R (1997) Sensitivity studies with the regional climate model REMO. Meteorol Atmos Phys 63: 119–129

Jacob D, den Hurk BJJMV, AndræG, Elgered G, Fortelius C, Graham LP, Jackson SD, Karstens U, Köpken C, Lindau R, Podzun R, Roeckel B, Rubel F, Sass BH, Smith RNB, Yang X (2001) A comprehensive model inter-comparison study investigation the water budget during the BALTEX-PIDCAP period. Meteorol Atmos Phys 77: 19–43

Jha B, Khrisnamurti TN, Christides Z (2000) A note on horizontal resolution dependence for monsoon rainfall simulations. Meteorol Atmos Phys 74: 11–17

Ji Y, Vernekar AD (1997) Simulation of the Asian summer monsoons of 1987 and 1988 with a regional model nested in a global GCM. J Clim 10: 1965–1979

Jones RG, Murphy JM, Noguer M (1995) Simulation of climate change over Europe using a nested regional climate model. I: assesment of control climate, including sensitivity to location of lateral boundaries. Q J R Meteorol Soc 121: 1413–1449

Kalnay E, Kanamitsu M, Kistler R, Collins W, Deaven D, Gandin L, Iredell M, Saha S, White G, Woollen J, Zhu Y, Chelliah M, Ebisuza W, Higgins W, Janowiak J, Mo KC, Ropelewski C, Wang J, Leetmaa A, Reynolds R, Jenne R, Joseph D (1996) The NCEP/NCAR 40-year reanalysis project. Bull Am Meteorol Soc 77: 437–471

Kesler E (1969) On the distribution and continuity of water substance in atmospheric circulations. Meteorolological Monograph 32, pp 84

Klemp JB, Durran DR (1983) An upper boundary condition permitting internal gravity wave radiation in numerical mesoscale models. Mon Weather Rev 111: 430–444

Laprise R, Varma MR, Denis B, Caya D, Zawadzki I (2000) Predictability of a nested limited area model. Mon Weather Rev 128: 4149–4154

Latif M, Flügel M (1991) An investigation of hot-range climate predictability in the tropical Pacific. J Geophys Res 96: 2661–2673

Latif M, Graham NE (1992) How much predictive skill is contained in the thermal structure of an OGCM? J Phys Ocean 22: 951–962

Latif M, Anderson DLT, Barnett TP, Cane MA, Kleeman R, Leetma A, O'Brien J, Rosati A, Schneider E (1998) A review of the predictability and prediction of ENSO. J Geophys Res 103: 14,375–14,393

Lorenz EN (1969) The predictability of a flow which possesses many scales of motion. Tellus 21: 289–307

Mc Gregor JL (1997) Regional climate modeling. Meteorol Atmos Phys 63: 105–117

Mc Gregor JL, Walsh K (1994) Climate change simulations of Tasmanian precipitation using multiple nesting. J Geophys Res 99: 20,889–20,905

Menendez CG, Saulo AC, Li Z (2001) Simulation of South American wintertime climate with a nesting system. Clim Dyn 17: 219–231

Mesinger F (1997) Dynamics of Limited-area models: formulation and numerical methods. Meteorol Atmos Phys 63: 3–14

Moore AM, Kleeman R (1996) The dynamics of error growth and predictability in a coupled model of ENSO. Q J R Meteorol Soc 122: 1405–1446

Morcrette JJ, Fouquart Y (1986) Pressure and temperature dependence of the absorption in longwave radiation parametrizations Beitr. Phys Atmos 59: 455–469

Nobre P, Moura AD, Sun L (2001) Dynamical downscaling of seasonal climate prediction over Nordeste Brazil with ECHAM3 and NCEP's regional sprectral model at IRI Bull Am Meteorol Soc 82: 2787–2796

Nordeng TE (1994) Extended versions of the convective parametrization scheme at ECMWF and their impact on the mean and transient activity of the model in the tropics., ECMWF Tech Mem 206, European Centre for Medium-range Weather Forecasts, Reading, UK

Nouger M, Jones RG, Murphy JM (1998) Sources of systematic errors in the climatology of a regional climate model over Europe. Clim Dyn 14: 691–712

Paegle J, Yang Q, Wang M (1997) Predictability in limited area and global models. Meteorol Atmos Phys 63: 53–69

Peterson TC, Vose R, Schmoyer R, Razuvaev V (1998) Global Historical Climatology Network (GHCN) quality control of monthly temperature data. Int J Clim 18: 1169–1179

Podzun R, Cress A, Majewski A, Renner V (1995) Simulation of European Climate with a limited area model. Part II. AGCM boundary conditions. Contrib Atmos Phys 68: 205–225

Rayner NA, Horton EB, Parker DE, Folland CK, Hackett RB (1996) Version 2.2 of the global sea-ice and sea surface temperature data set, 1903–1994. Tech Note CRTN74 Climate Research, pp 35

Roeckner E, Arpe K, Bengston L, Christoph M, Claussen M, Dumenil L, Esch M, Giorgetta M, Schlese U, Schulzweida U (1996) The atmospheric general circulation model ECHAM-4: model description and simulation of present-day climate. MPI Report 218, Max Planck-Institut für Meteorologie, Bundesstr. 55, D-20146, Hamburg, Germany pp 90

Simmons AJ, Burridge DM (1981) An energy and angular-momentum conserving vertical finite-difference scheme and hybrid vertical coordinates. Mon Weather Rev 109: 758–766

Staniforth A (1997) Regional modeling: a theoretical discussion. Meteorol Atmos Phys 63: 15–29

Stendel M, Roeckner E (1998) Impacts of horizontal resolution on simulated climate statistics in ECHAM4. MPI Rep 253, Max Planck-Institut für Meteorologie, Bundesstr. 55, D-20146, Hamburg, Germany pp 57

Sundqvist H (1978) A parametrization scheme for non-convective condensation including prediction of cloud water content. Q J R Meteorol Soc 104: 677–690

Thompson CJ, Battisti DS (2001) A linear stochastic dynamical model of ENSO. Part II: analysis. J Clim 14: 445–466

Tiedtke M (1989) A comprehensive mass flux scheme for cumulus parametrization in large scale models. Mon Weather Rev 117: 1779–1800

Vose RS, Schmoyer RL, Steurer PM, Peterson TC, Heim R, Karl TR, Eischeid JK (1992) The Global Historical Climatology Network: long-term monthly temperature, precipitation, sea level pressure, and station pressure data. ORNL/CDIAC-53 NDP-041 pp 325

Vukicevic T, Errico RM (1990) The influence of artificial and physical factors upon predictability estimates using a complex limited area model. Mon Weather Rev 118: 1460–1482

Warner TT, Peterson RA, Treadon RE (1997) A tutorial on lateral boundary conditions as a basic and potentially serious limitation to regional numerical weather prediction. Bull Am Meteorol Soc 78: 2599–2617

Webster PJ, Yang S (1992) Monsoon and ENSO: selectively interactive systems. Q J R Meteorol Soc 118: 877–925

Weiss JP, Weiss JB (1999) Quantifying persistence in ENSO. J Atmos Sci 56: 2737–2760

Yu ZP, Chu PS, Schroeder T (1997) Predictive skills of seasonal to annual rainfall variations in the US affiliated Pacific Islands: canonical correlation analysis and multivariate principal component regression approaches. J Clim 10: 2586–2599